Quaternarized pdppz: Synthesis, DNA-binding and biological studies of a novel dppz derivative that causes cellular death upon light irradiation

Robert B. P. Elmes,[a] Marialuisa Erby,[b] Suzanne M. Cloonan,[b] Susan J. Quinn,[c*] D. Clive Williams[b]* and Thorfinnur Gunnlaugsson[a]*

[a] *School of Chemistry, Centre for Synthesis and Chemical Biology, Trinity College Dublin, Dublin 2, Ireland. Fax: +353 1671 2826; Tel: + 353 1 896 3459; E-mail:* gunnlaut@tcd.ie.

[b]*School of Biochemistry and Immunology, Trinity College, Dublin 2, Ireland E-mail: clive.williams@tcd.ie, Fax: +353 1 8963130; Tel: + 353 1 8962596.*

[c]*School of Chemistry and Chemical Biology, Centre for Chemical Synthesis and Chemical Biology, UCD, Dublin 4, Ireland., University College Dublin, Belfield, Dublin 4, Ireland*

General experimental procedures and characterisation

All NMR spectra were recorded using either a 400 MHz using a Bruker Spectrospin DPX-400 or AV-600 spectrometer, operating at 400.1/ 600.1 MHz for ^{1}H NMR and 100.2/150.2 MHz for ^{13}C NMR respectively. Shifts are referenced relative to the internal solvent signals. Electrospray mass spectra were recorded on a Micromass LCT spectrometer, running Mass Lynx NT V 3.4 on a Waters 600 controller connected to a 996 photodiode array detector with HPLC-grade methanol or acetonitrile. High resolution mass spectra were determined by a peak matching method, using leucine Enkephalin, (Tyr-Gly-Gly-Phe-Leu), as the standard reference (m/z = 556.2771). All accurate mass were reported within ±5 ppm. Melting points were determined using an IA9000 digital melting point apparatus. Infrared spectra were recorded on a Perkin Elmer Spectrum One FT-IR spectrometer fitted with a Universal ATR Sampling Accessory. Elemental analysis was conducted at the Microanalytical Laboratory, School of Chemistry and Chemical Biology, University College Dublin.

UV-visible absorption spectra were recorded on a Varian Cary 50 spectrometer. Emission spectra were recorded on a Cary Eclipse Luminescence spectrometer. The luminescence quantum yields were calculated using Quinine Sulphate in 0.1 N H_2SO_4 with a quantum yield of 0.542 as a reference. Linear dichroism (LD) spectra were recorded at a concentration corresponding to an optical density of approximately 2.5, in buffered solutions, on a Jasco J-810-150S spectropolarimeter.

Solutions of Salmon testes (st) DNA in 10 mM phosphate buffer (pH 7.4) gave a ratio of UV absorbance at 260 and 280 nm of 1.86:1, indicating that the DNA was sufficiently free of protein. Its concentration was determined spectrophotometrically using the molar absortivity of 6600 M^{-1} cm^{-1} (260nm). Titrations were carried out by monitoring changes in the absorbance and emission spectra of the dye, **1** (10 μM) at pH 7.4 in 10 mM phosphate

buffer upon successive additions of aliquots of stDNA. The results are quoted using the concentration of stDNA expressed as a nucleotide phosphate to dye ratio (P/D ratio)

6-nitroquinoxaline

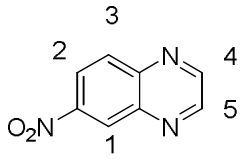

4-nitrobenzene-1,2-diamine (4 g, 27.95 mmol, 1 eq.) was suspended in EtOH (100 ml) before an aqueous solution of oxalaldehyde (40%, 6 ml) was added and the mixture heated at reflux for 2 hrs. The solvent was removed under reduced pressure before being dissolved in water (200 ml) and the aqueous layer extracted with DCM (4 x 50 ml). The solvent was again removed under reduced pressure after being dried over $MgSO_4$. The resulting orange solid was recrystallised twice from isopropanol (2 x 150 ml) to yield golden crystalline needles (4.07 g, 83%). **δ_H (400 MHz, [D_6] DMSO):** 8.36 (d, 1H, J=9.04 H-3), 8.57 (dd, 1H, J=2.52, J=9.04, H-2), 8.91 (d, 1H, J=2.52, H-1), 9.17 (s, 2H, H-4 and H-5). **δ_C (100 MHz, [D_6] DMSO)**: 123.56, 125.25, 131.26, 140.99, 144.66, 147.60, 148.13, 148.87. **ν_{max} (film)/cm^{-1}:** 1520 (C-NO_2), 1344 (C-NO_2). **HRMS (*m/z* -ES)** : Found: 176.0474 (M+H. $C_8H_6N_3O_2$ Requires: 176.0460).

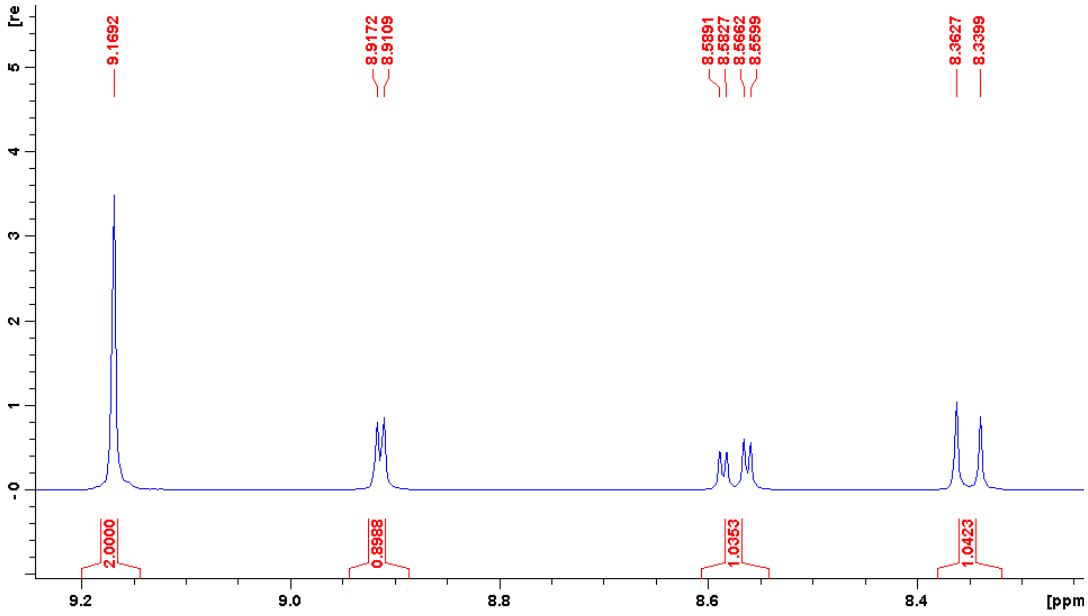

Figure ESI 1: ^{1}H (400 MHz) NMR of **6-nitroquinoxaline** in [D_6] DMSO

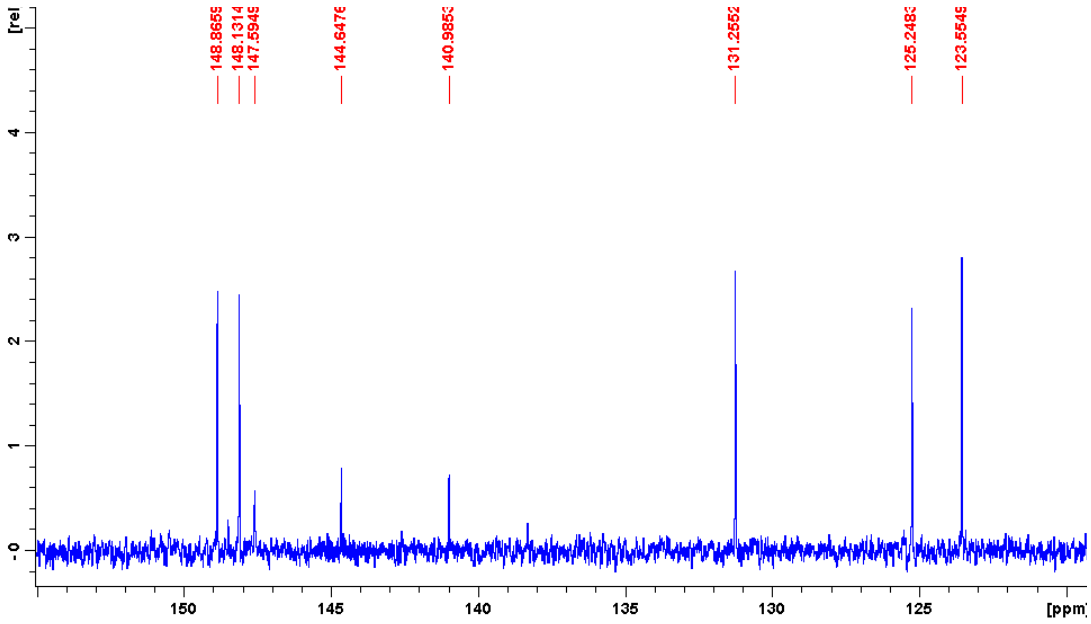

Figure ESI 2: ^{13}C (100 MHz) NMR of **6-nitroquinoxaline** in [D_6] DMSO

6-nitroquinoxalin-5-amine

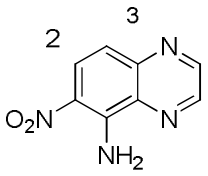

Sodium metal (2.3 g, 100 mmol, 3.3 eq.) was added to distilled MeOH (125 ml). A solution of hydroxylamine (3.13 g, 45 mmol, 1.5 eq.) in distilled MeOH (50 ml) was added after cooling to 0° C on ice. The resulting NaCl precipitate was allowed to settle before the supernatant solution was added to a well stirred suspension of 6-nitroquinoxaline in boiling MeOH (250 ml). The resulting brown reaction mixture was heated under reflux for 90 mins before being cooled to 0° C on ice. The resulting yellow precipitate was collected by suction filtration before being recrystallised from a mixture of acetic acid and water (3:1, 150 ml) to yield bright yellow crystalline needles (2.49 g, 43%). **δ_H (400 MHz, [D_6] DMSO):** 7.19 (d, 1H, J=9.52, H-3), 8.30 (d, 1H, J=9.52, H-2), 8.53 (s, 2H, NH_2) 8.94 (d, 1H, J=2.04, H-4/5), 9.10 (d, 1H, J=2.00, H-4/5). **δ_C (100 MHz, [D_6] DMSO)**:114.34, 126.11, 134.16, 143.22, 145.09, 145.84, 148.85. **ν_{max} (film)/cm^{-1}:**3297 (N-H Stretch), 1615 (N-H bend), 1520 (C-NO_2), 1344 (C-NO_2). **HRMS (*m/z* -ES)** : Found: 191.0568 (M+H. $C_8H_7N_4O_2$ Requires: 191.0569).

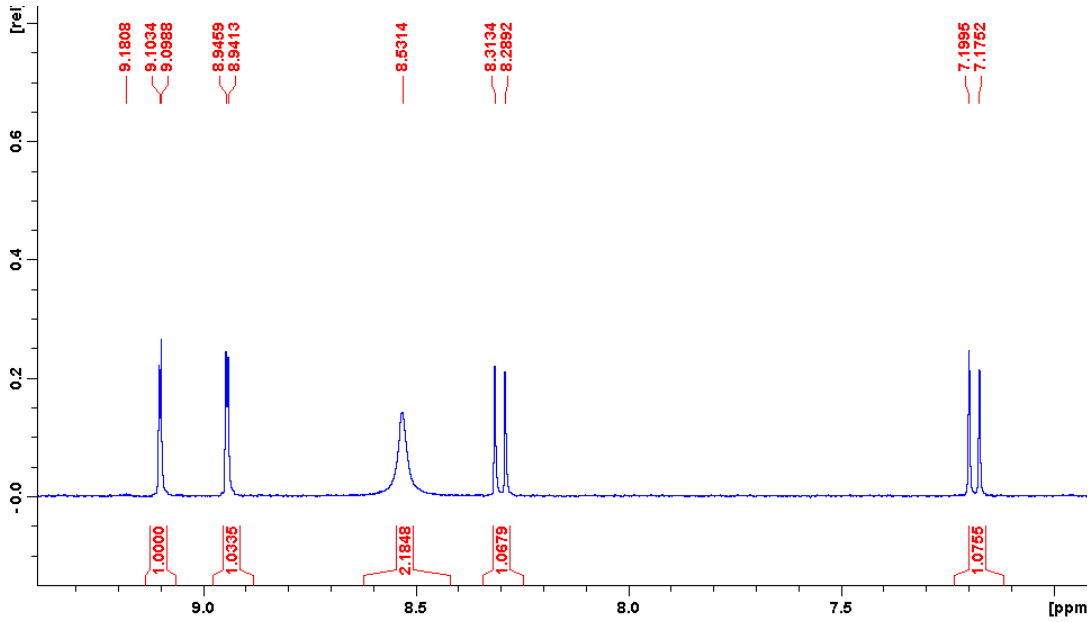

Figure ESI 3: ^{1}H (400 MHz) NMR of **6-nitroquinoxalin-5-amine** in [D_6] DMSO

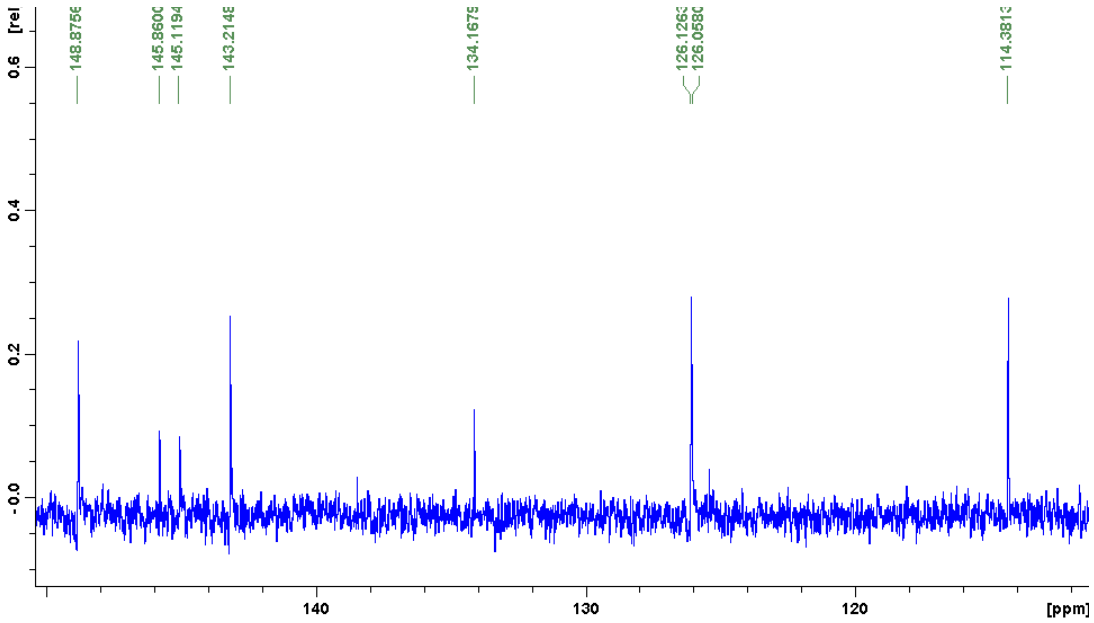

Figure ESI 4: ^{13}C (100 MHz) NMR of **6-nitroquinoxalin-5-amine** in [D_6] DMSO

quinoxaline-5,6-diamine

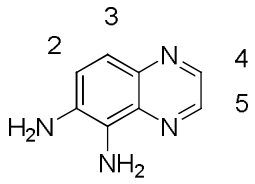

6-nitroquinoxalin-5-amine (1.5 g, 7.86 mmol, 1 eq.) and 10% Pd/C (0.2 g) were added to EtOH (80 ml) and the mixture heated at reflux for 1 hr. Hydrazine monohydrate (98%, 7.89 g, 157.6 mmol, 20 eq) was added and the mixture was again heated at reflux for 1 hr. The resulting red/black mixture was filtered hot through a pad of celite and the solid washed with DCM (80 ml). The solvent was removed under reduced pressure yielding a blood red solid which was dried under high vacuum (1.24 g, 98%). m.p.147-148°C. **δ_H (400 MHz, [D_6] DMSO):** 5.16 (s, 2H, NH_2), 5.28 (s, 2H, NH_2), 7.20 (d, 1H, J=8.52, H-2/3), 7.26 (d, 1H, J=9.04, H-2/3), 8.51 (d, 1H, J=2.00, H-4/5), 8.58 (d, 1H, J=2.00, H-4/5) **δ_C (100 MHz, [D_6] DMSO)**: 116.33, 121.80, 126.04, 132.4082, 133.03, 136.92, 140.12, 141.9037. **ν_{max} (film)/cm^{-1}**: 3306 (N-H Stretch), 1610 (N-H bend). **HRMS (*m/z* -ES)** : Found: 161.0816 (M+H. $C_8H_9N_4$ Requires: 161.0827).

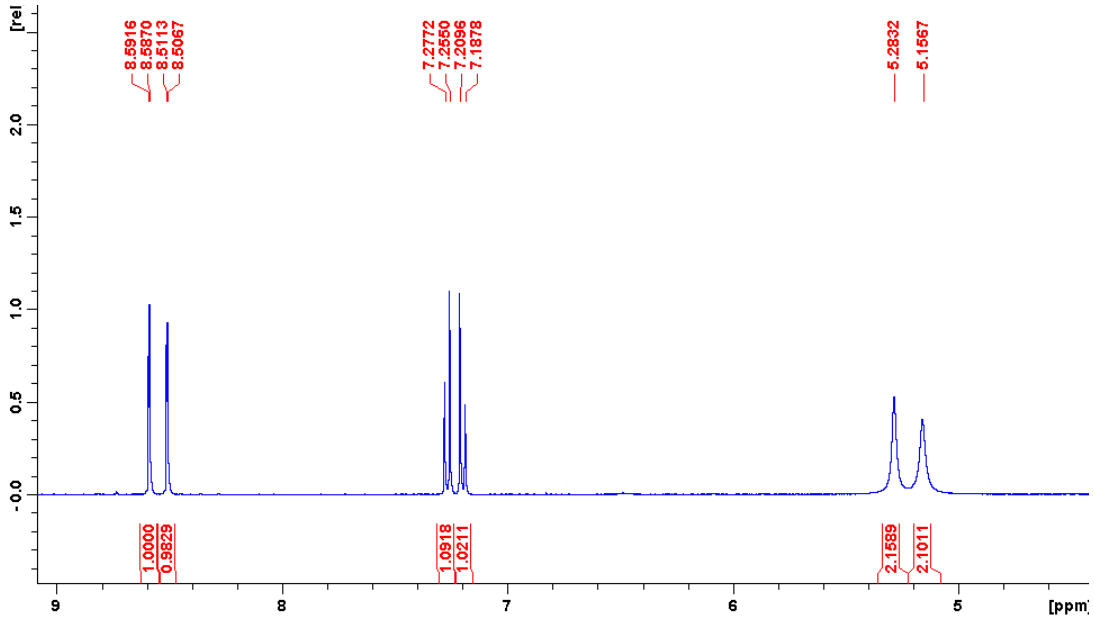

Figure ESI 5: ^{1}H (400 MHz) NMR of **quinoxaline-5,6-diamine** in [D_6] DMSO

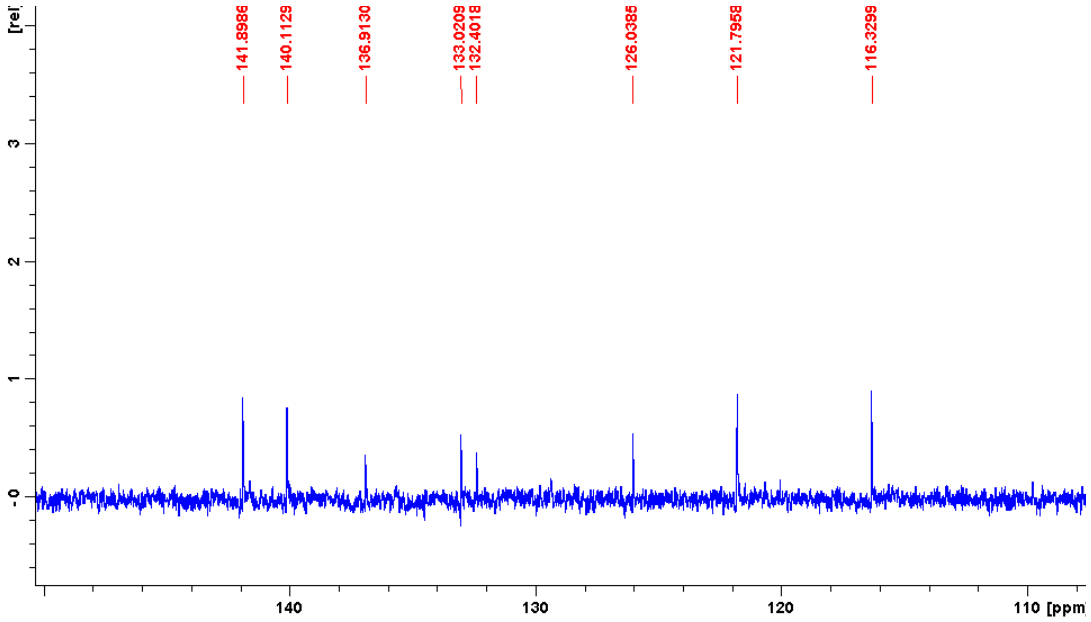

Figure ESI 6: ^{13}C (100 MHz) NMR of **quinoxaline-5,6-diamine** in [D_6] DMSO

Pyrazino[2,3-h]dipyrido[3,2-a:2',3'-c]phenazine

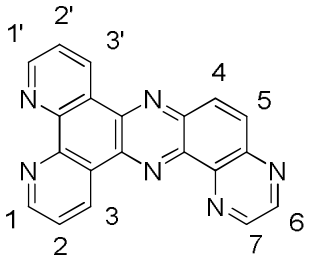

Quinoxaline-5,6-diamine (0.1 g, 0.476 mmol, 1 eq.) and 1,10-phenanthroline-5,6-dione (0.084 g, 0.524 mmol, 1.1 eq.) were suspended in a mixture of EtOH and water (1:1, 15 ml) and heated at 140° C in a pressure tube overnight. The resulting brown precipitate was collected by suction filtration, washed with water (10 ml), EtOH (10 ml) and Et_2O (15 ml) before being dried under high vacuum. The product was obtained as a grey solid (0.151 g, 95%). m.p. >250 °C **.**Calculated for $C_{20}H_{10}N_6.0.5H_2O$: C, 69.96; H, 3.23; N, 24.48. Found: C, 69.25; H, 3.24; N, 24.2. m.p. >250 °C, **δ_H (600 MHz, [D_6] DMSO):** 8.10 (m, 2H, H-2 and H-2'), 8.52 (d, 1H, J=9.12, H-4/5), 8.63 (d, 1H, J=9.42, H-4/5), 9.30 (d, 1H, J= H-3/H-3'), 9.32 (m, 2H, H-7 and H-6'), 9.38 (d, 1H, J=1.74, H-3/3'), 9.70 (d, 1H, J=9.36, H-1/1'), 9.82 (d, 1H, J=7.62, H-1/1'). **ν_{max} (film)/cm^{-1}:** 3258 (Aromatic C-H stretch), 1378 (C-N stretch). **HRMS (*m/z* -ES)** : Found: 335.1048 (M+H. $C_{20}H_{11}N_6$ Requires: 335.1045).

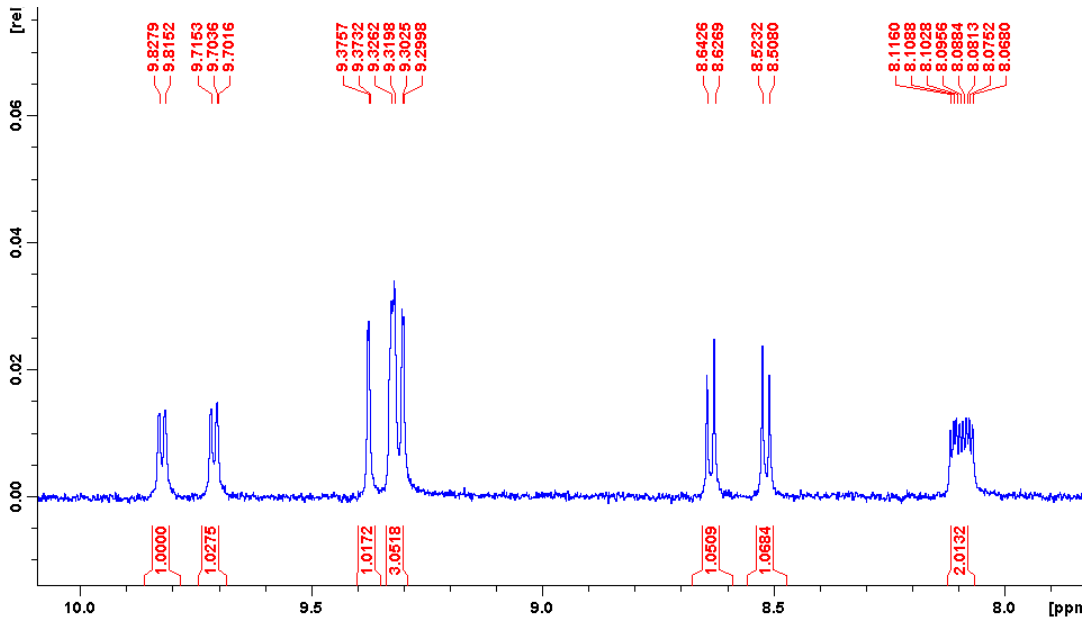

Figure ESI 7: ^{1}H (400 MHz) NMR of **Pyrazino[2,3-h]dipyrido[3,2-a:2',3'-c]phenazine** in [D_6] DMSO

Pyrazino[2,3-h]ethylenedipyrido[3,2-a:2',3'-c]phenazilium dichloride

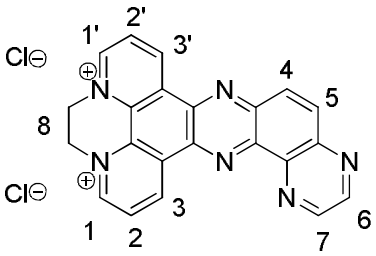

Pyrazino[2,3-h]dipyrido[3,2-a:2',3'-c]phenazine (0.17 g, 0.5 mmol, 1 eq.) was suspended in dibromoethane (25 ml) before the suspension was heated at 135° C for 24 hrs. The resulting brown precipitate was isolated by suction filtration before the chloride form of the complex was formed by stirring a solution of the bromide complex in MeOH (35 ml) with Amberlite ion exchange resin (chloride form) for 1 hr. The solution was filtered and reduced in volume before being precipitated from solution by slow addition of diethyl ether. The resulting precipitate was isolated by suction filtration and washed with diethyl ether (2 x 10 ml) yielding a brown solid (0.17 g, 78%). %).Calculated for $C_{22}H_{14}N_6Cl_2.5H_2O$: C, 50.48; H, 4.62; N, 16.06. Found: C, 50.46; H, 4.17; N, 16.04. m.p. >250 °C, **δ_H (600 MHz, MeOD):** 11.21 (dd, 1H, J=1.24, J=8.48, H-1/H-1'), 10.76 (dd, 1H, J=1.12, J=8.44, H-1/H-1'), 9.89 (dt, 2H, J=5.04, J=5.92, H-3 + H3'), 9.41 (s, 2H, H-6 + H-7), 8.95 (m, 2H, H-2 + H-2'), 8.85 (AB sys, 2H, J_{AB}=9.48, H-4 + H-5), 5.85 (s, 4H, H-8). **δ_C (100 MHz, [D_6] DMSO)**: 150.19, 149.96, 148.89, 146.53, 146.08, 146.07, 145.18, 144.46, 142.90, 140.56, 139.00, 137.78, 136.02, 132.87, 132.72, 132.63, 132.18, 131.84, 129.65, 129.64, 53.08, 53.06. **ν_{max} (film)/cm^{-1}:** 3258 (Aromatic C-H stretch), 1378 (C-N stretch). **HRMS (*m/z* -ES)** : Found: 393.1446 ($M^{2+}MeO^-$) $C_{23}H_{17}N_6O_2$ Requires: 393.1453).

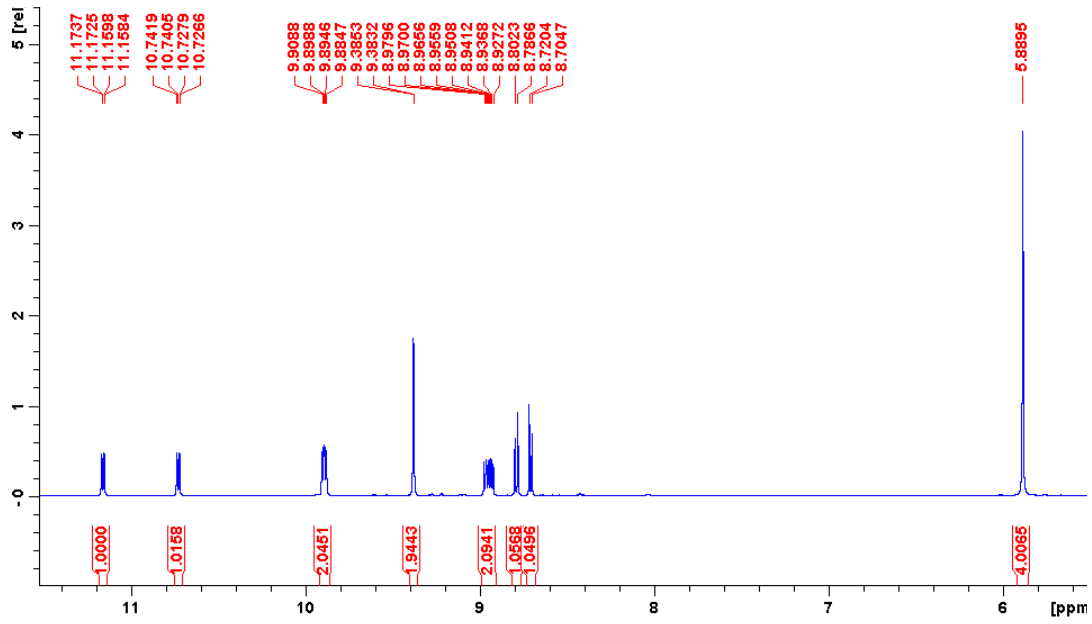

Figure ESI 8: ^{1}H (400 MHz) NMR of **Pyrazino[2,3-h]ethylenedipyrido[3,2-a:2',3'-c]phenazilium dichloride** in [D_6] DMSO

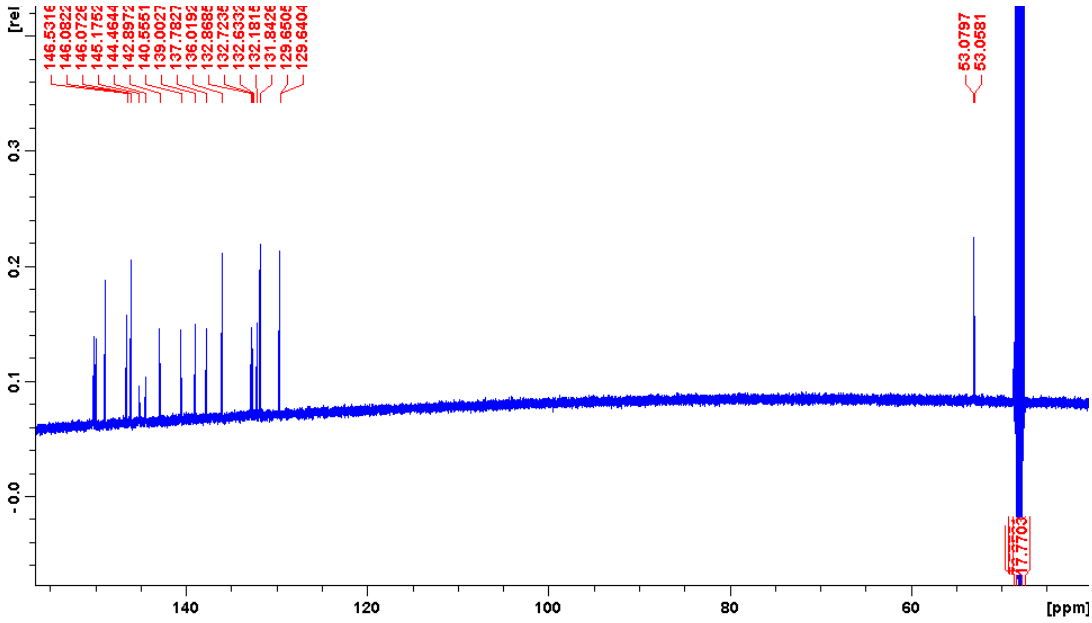

Figure ESI 9: ^{13}C (100 MHz) NMR of **Pyrazino[2,3-h]ethylenedipyrido[3,2-a:2',3'-c]phenazilium dichloride** in [D_6] DMSO

Calculation of binding constants from UV/Vis Titration Data

The intrinsic binding constant K_b, and binding site size *n* were determined using the model of Bard *et al*.,[1] equation **(1)** from a plot of $(\varepsilon a-\varepsilon f)/(\varepsilon b-\varepsilon f)$ vs. $[DNA]$. εa, εf, εb correspond to the apparent extinction coefficient, the extinction coefficient for the free dye, and the extinction coefficient for the dye in the fully bound form. C_t is the total dye concentration, $[DNA]$ is the DNA concentration expressed in nucleotide phosphate, and n is the binding site size. The data was fit to this model using non-linear regression with Sigmaplot 11.0.

$$\frac{(\varepsilon_a-\varepsilon_f)}{(\varepsilon_b-\varepsilon_f)} = \frac{[b-(b^2-2K_b+C_t[DNA]/n)^{1/2}]}{(2K_bC_t)} \quad \textbf{(1)}$$

$$b = 1 + K_b C_t + K_b[DNA]/2 \quad \textbf{(2)}$$

Calculation of binding constants from Fluorescence Titration Data

K_b was determined from both the absorbance and luminescence data according to the McGhee and Von Hippel model.[2] The concentration of the bound compound C_b, and free compound C_f, at a given concentration were firstly determined from equations **(3)** and **(4)**:

$$C_b = \frac{I_f-I}{I_f-I_b} \cdot C \quad \textbf{(3)}$$

$$C_f = C - C_b \quad \textbf{(4)}$$

Here I_f and I_b are the fluorescence intensities of the free and bound compound, I is the fluorescence response and C is the dye concentration. The absorbance data was treated in a similar manner. Data analysis was then carried out as described in equation **(5)**, where, $r = C_b/[DNA]$, ($[DNA]$ is the concentration of DNA expressed in base pairs). Analysis was achieved using the plot of r/C_f versus r and the curve was fit to equation **(5)** using Sigmaplot 11.0.

$$\frac{r}{C_f} = K_b(1-nr)\left(\frac{1-nr}{1-(n-1)r}\right)^{n-1} \quad \textbf{(5)}$$

Calculation of binding constant from ethidium bromide displacement assays

The apparent binding constant K_{app} were calculated according to the competitive binding model described by Tse and Boger [3] using equation **(6)**:

$$K_{app} = K_{EB}[EB]/[agent] \qquad (6)$$

where K_{EB} is the binding constant for ethidium bromide, ***[EB]*** is the concentration of ethidium bromide and ***[agent]*** is the dye concentration at 50% of the fluorescence.

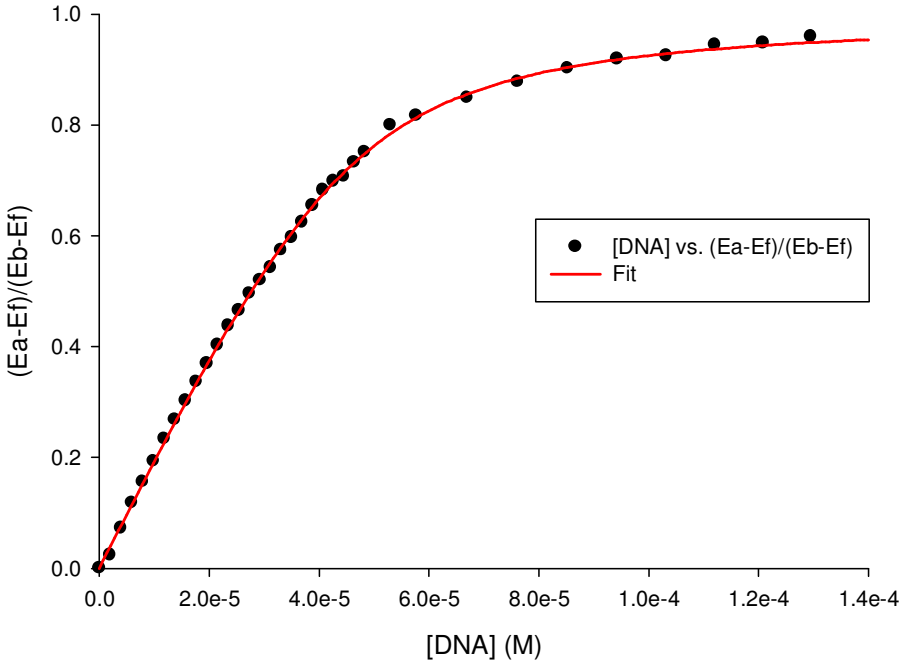

Figure ESI 10: Plot of $(\varepsilon_a-\varepsilon_f)/\varepsilon_b-\varepsilon_f)$ vs. **[DNA]**(M^{-1}, Bp) using data with a P/D between 0-10 and the best fit of the data (---) using the Bard Eqn.

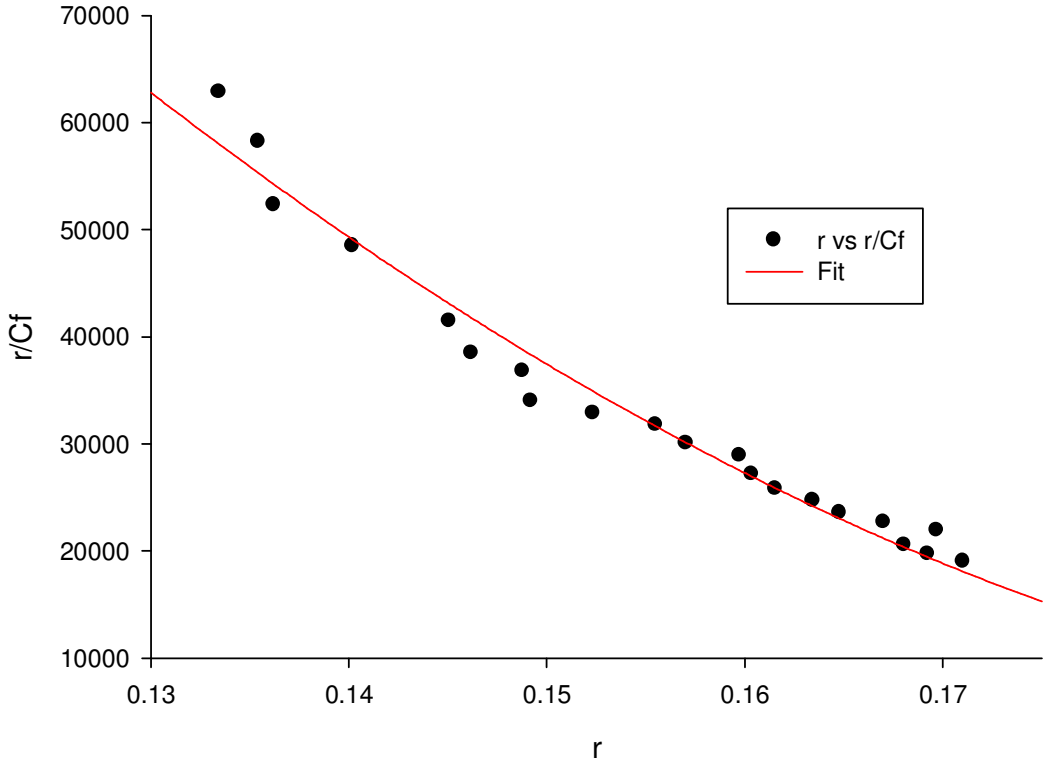

Figure ESI 11: Scatchard plot (●) and the best fit of the emission data (---) for **1** in 10 mM phosphate buffer according to the model of Mc Ghee and Von Hippel, equation **(5)**.

	Hypochromicity	**Bard Binding Constant**	**Bard Binding Site Size**	**Bard R^2**	**McGhee Binding Constant**	**McGhee Binding Site Size**	**McGhee R^2**
stDNA	52%	6.5×10^5 (± 0.5)	2.6 (± 0.03)	0.998	3.55×10^5 (± 0.02)	4.05 (± 0.05)	0.970
Poly dG-dC	54%	1.35×10^7 (± 0.55)	1.67 (± 0.05)	0.998	1.84×10^7 (± 0.1)	1.35 (± 0.01)	0.998
Poly dA-dT	51%	4.85×10^5 (± 0.33)	3.91 (± 0.01)	0.999	5.60×10^5 (± 0.27)	3.3 (± 0.05)	0.993

Table ESI 1: DNA binding parameters from fits to absorbance data using both the Bard and McGhee Von Hippel equations

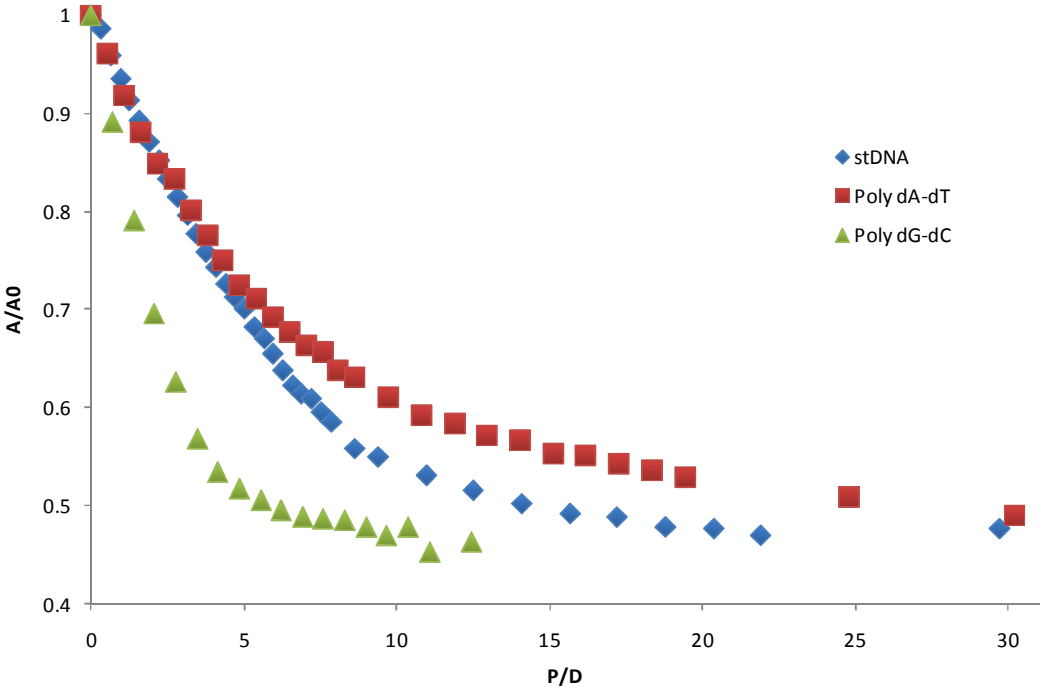

Figure ESI 12: Relative changes in the absorbance of **1** (10 µM) with increasing concentration of stDNA, (◆) (0-172µM), $[Poly(dAdT)]_2$,(■) (0-175µM), and $[Poly(dGdC)]_2$, (▲) (0-63µM) in 10 mM phosphate buffer.

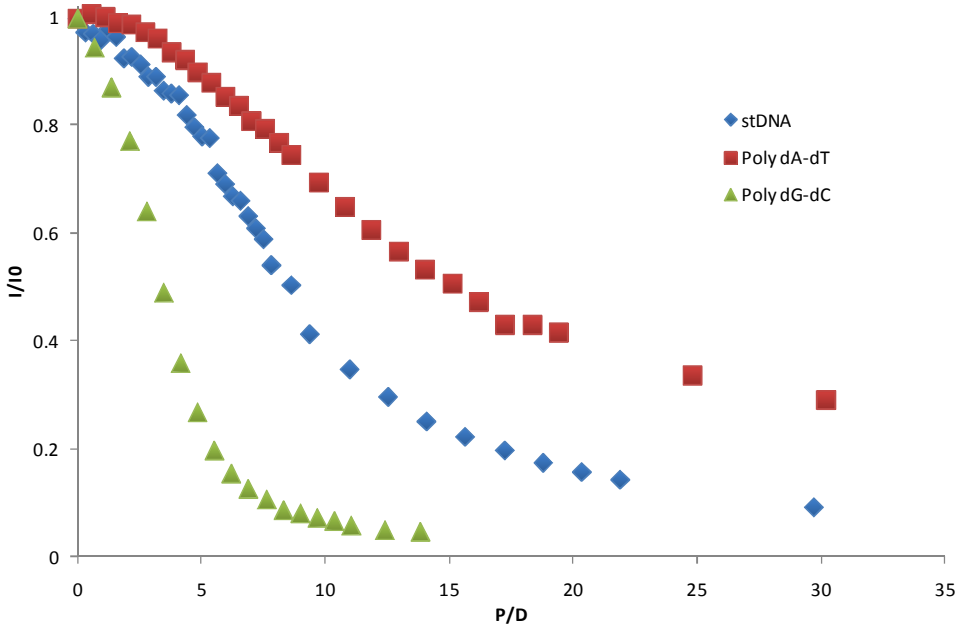

Figure ESI 13: Relative changes in the emission of **1** at 515 nm (10 µM) with increasing concentration of stDNA, (◆) (0-172µM), $[Poly(dAdT)]_2$,(■) (0-175µM), and $[Poly(dGdC)]_2$, (▲) (0-63µM) in 10 mM phosphate buffer.

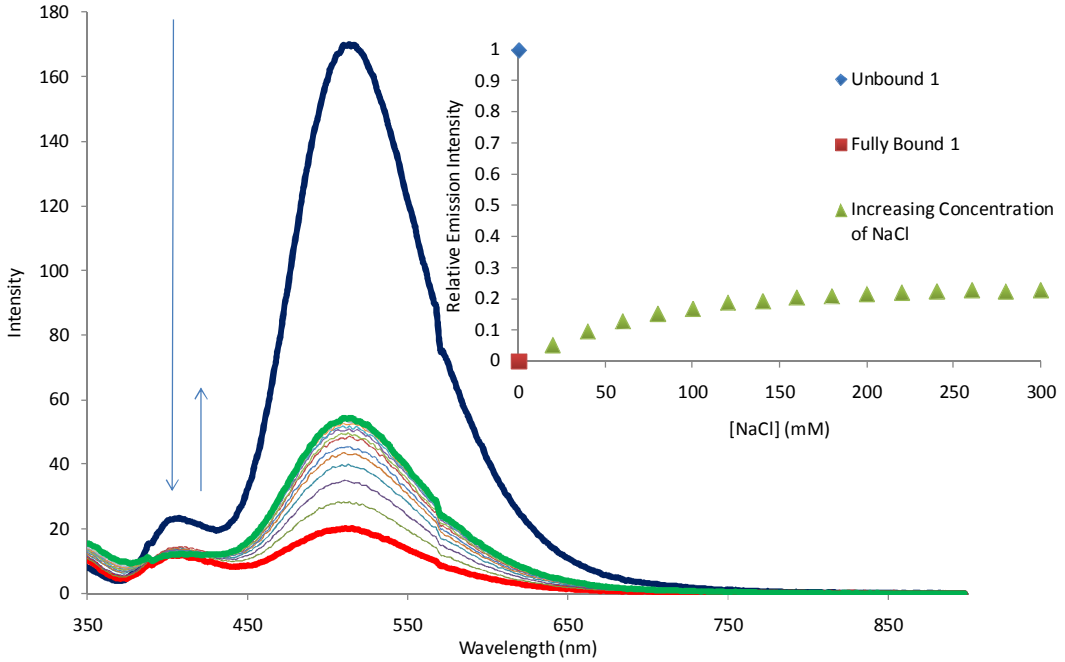

Figure ESI 14: Fluorescence emission NaCl back titration of **1**. Emission of unbound compound (◆), fully bound compound (■) and bound compound in the presence of increasing concentration of NaCl(▲)

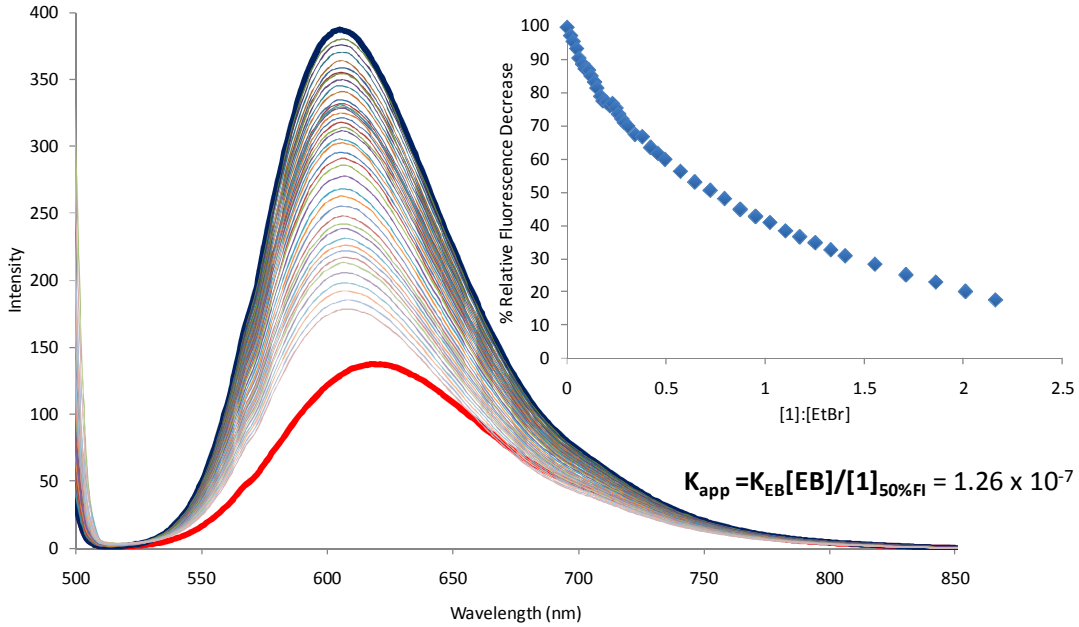

Figure ESI 15: Emission changes for DNA bound EtBr (λ_{ex} 545 nm) with increasing concentration of **1** in 10 mM phosphate buffer at pH 7.4. **Inset.** Relative decrease in fluorescence of DNA bound EtBr upon addition of **1**

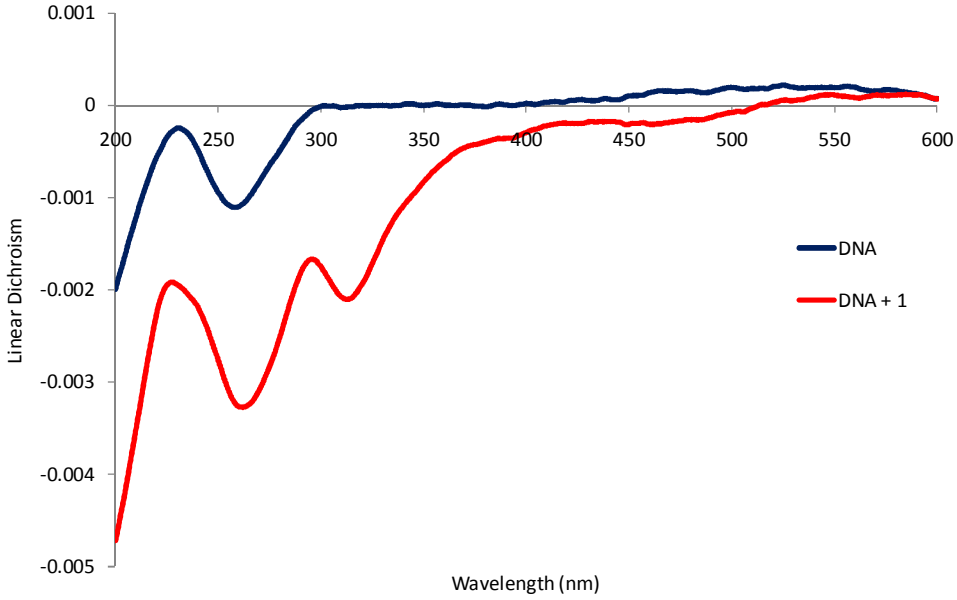

Figure ESI 16: Linear dichroism curves of stDNA (750 µM) in 10 mM phosphate buffer, at pH 7.4, in the absence and presence of **1** (P/D 2.5)

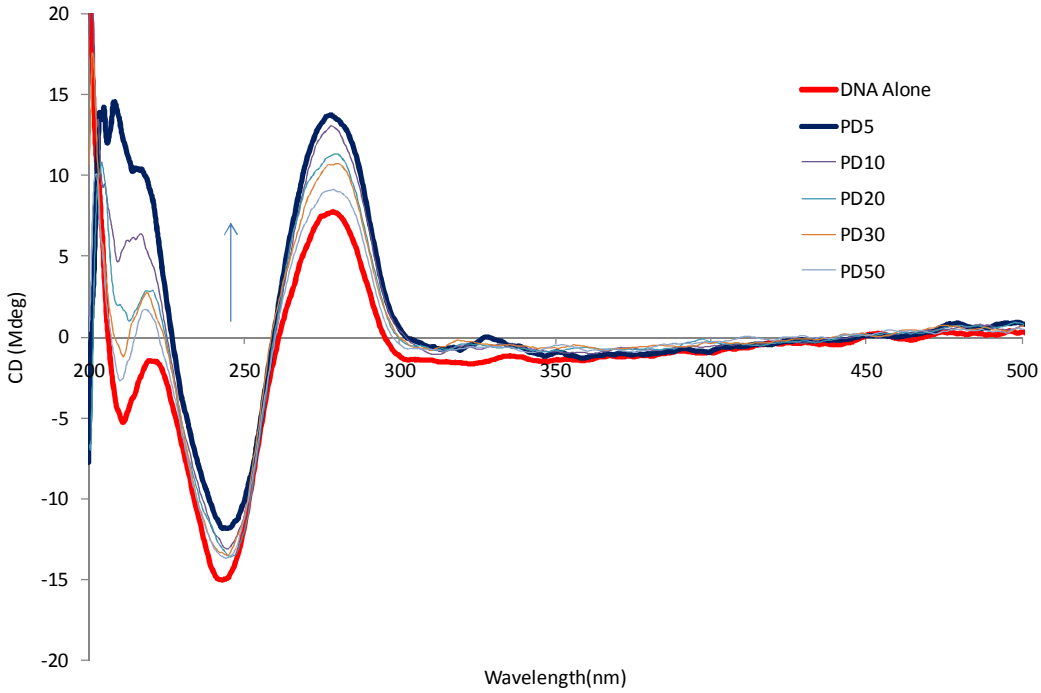

Figure ESI 17: Circular dichroism spectra of stDNA (150 µM) in 10 mM phosphate buffer at pH 7.4 in the absence and presence of **1** at varying P/D ratios

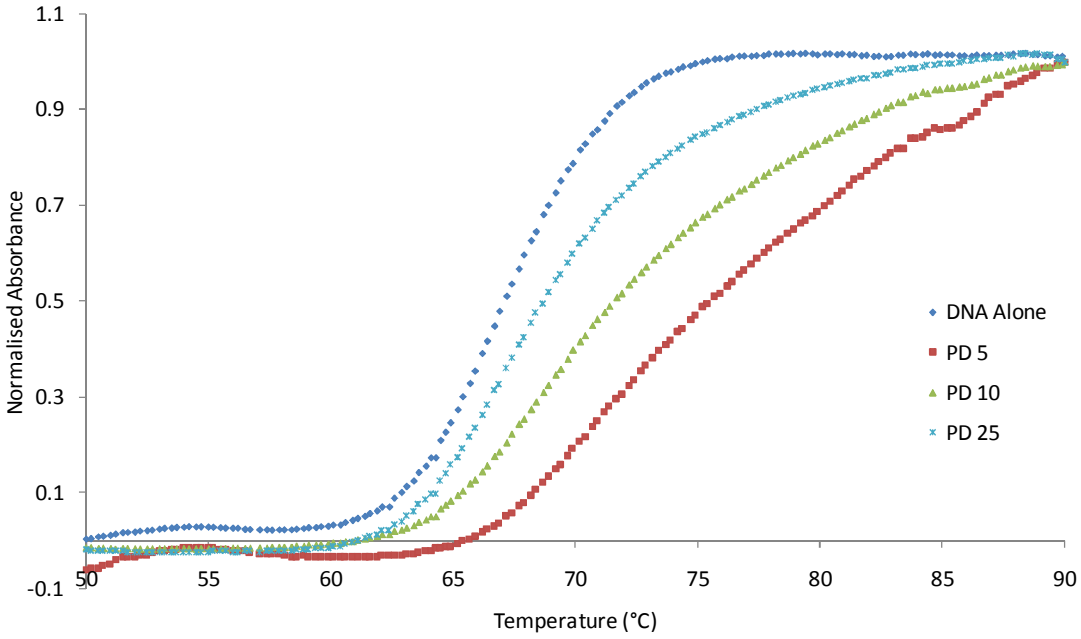

Figure ESI 18: Thermal denaturation curves of stDNA (150 µM) in 10 mM phosphate buffer at pH 7.4 in the absence and presence of **1** at varying P/D ratios

	T_m
StDNA	67°C
1 (P/D 25)	72°C
1 (P/D 10)	>75°C
1 (P/D 5)	>75°C

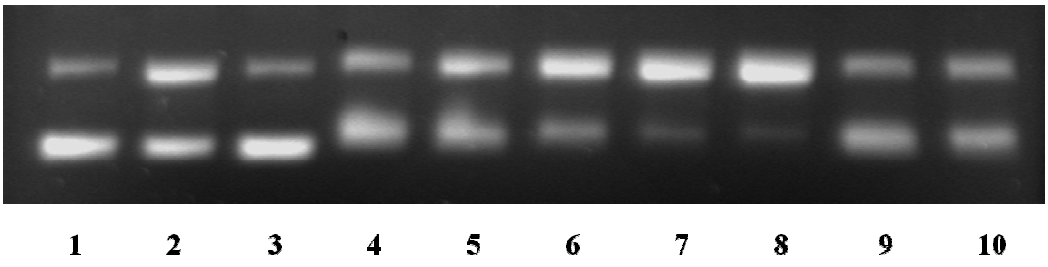

Figure ESI 19: Agarose gel electrophoresis of pBR322 DNA (1mg/ml) after 30 min irradiation (2 J cm^{-1}) in 10 mM phosphate buffer, pH 7. 4; Lane 1: Plasmid DNA control ;Lane 2: $Ru(bpy)_3^{2+}$ (P/D 20); Lane 3:NaN_3 Control; Lane 4 : **RE33** in the dark (P/D 10); Lanes 5-6: **RE33** (P/D 20, 10) (λ > 400 nm); Lanes 7-8: **RE33** (P/D 20, 10) (λ > 320 nm); Lanes 9-10: **RE33 + 10mM NaN_3** (P/D 20, 10).

Lane	% Open	% Supercoiled
1	19.2	80.8
2	54.76	45.24
3	18.47	81.53
4	33.12	66.88
5	45.70	54.30
6	73.91	26.09
7	90.35	9.65
8	96.07	3.93
9	35.85	64.15
10	45.81	54.19

Table ESI 2: Percentage open circular vs. supercoiled pBR322 plasmid DNA from the agarose gel electrophoresis study

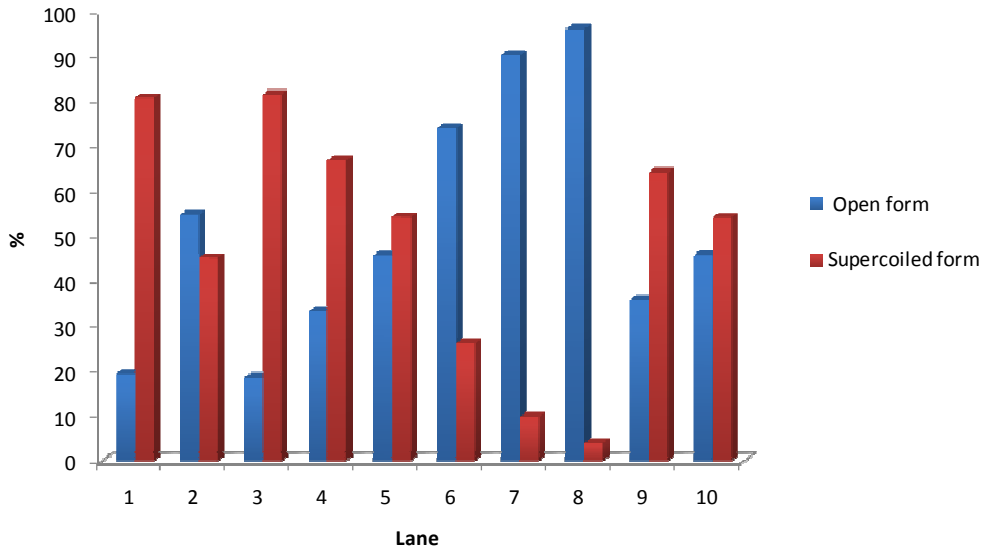

Figure ESI 20: Comparison of the percentage of open circular *vs.* supercoiled pBR322 plasmid DNA from the agarose gel electrophoresis study

1. Carter, M. T.; Rodriguez, M.; Bard, A. J. *J. Am. Chem. Soc.* **1989**, *111*, 8901-8911.
2. McGhee, J. D.; Hippel, P. H. V. *J. Mol. Biol.* **1974**, *86*, 469-489.
3. Boger, D. L.; Fink, B. E.; Brunette, S. R.; Tse, W. C.; Hedrick, M. P. *J. Am. Chem. Soc.* **2001**, *123*, 5878-5891.